

Optimizing Random Fourier Sampling Patterns for Compressed Sensing Using Point Spread Functions

David S Smith¹, Lori R Arlinghaus¹, Thomas E Yankeelov¹, and E Brian Welch¹
¹Institute of Imaging Science, Vanderbilt University, Nashville, TN, United States

INTRODUCTION One barrier to the clinical adoption of compressed sensing (CS) MRI (1) is the lack of predictability of the reconstructed image quality when the sampling pattern is random and the sampled anatomy is unknown and possibly highly variable. In many clinical imaging methods, the imaging system's spatial frequency response serves as a quality predictor (e.g., the modulation transfer function in mammography and fluoroscopy.) Unfortunately, the images reconstructed from a CS MRI algorithm are nonlinear functions of the compressively sampled data, so the point spread function (PSF) of the system is not simply related by the convolution theorem to the sampling pattern. However, it is simply related to the "minimum energy" reconstruction, in which missing data are replaced with zeros in the Fourier domain. Motivated by this connection, we explored the effect of the PSF of the random undersampling pattern on the ultimate quality of CS MRI reconstructions of a T_1 -weighted image of the breast.

MATERIALS AND METHODS A full Nyquist sampled complex T_1 -weighted breast image (dimension 192^2 , signal-to-noise 32.4) acquired on a Philips Achieva 3T scanner (Philips Healthcare, Best, The Netherlands) using a 16-channel Mamotrak breast coil was chosen as the ground truth. The fully sampled Fourier data were created by forward transforming this complex image. One third of the full data set was then sampled by 1000 different random Cartesian undersampling patterns. A point spread function (PSF) was calculated from each random sampling pattern, and a corresponding TV-minimized CS reconstruction was performed using the algorithm of Goldstein & Osher (2). Finally, the normalized mean square error (NMSE) of each CS reconstruction was compared to the various features of the mask PSF, including the variance, FWHM, and kurtosis.

RESULTS Fig. 1 shows the example images from the CS reconstructions. The left image should be compared to the middle and right, which represent the CS reconstructions using the sampling patterns with the maximum and minimum variance PSFs, respectively. Fig. 2 shows the shape of the mask PSF for the minimum variance (blue) and maximum variance (red) masks. Little difference can be seen except for a slight difference in peak width and power at low frequencies. Fig. 3 shows the NMSE of each CS reconstruction compared to the variance of the PSF of the associated sampling pattern. The graph clearly shows that larger mask PSF variance produces a more accurate reconstruction. The Spearman correlation coefficient was -0.55 ($p < 10^{-80}$). Also, the absolute level of error appears predictably low for the largest variance PSFs. We also found a similar result using the PSF kurtosis and FWHM, but with weaker correlations.

DISCUSSION Despite the nonlinear and random nature of the CS reconstruction and the spatially variant PSF, a reliable predictor of the ultimate reconstruction quality using a measure independent of the acquired data is available; i.e., the CS sampling mask PSF variance. Furthermore, the difference in quality of the two CS reconstructions in Fig. 1 (middle, right) show that significant improvement in image quality may be obtained by optimizing this data-independent quantity before the acquisition. Future work will extend this idea to 3D Cartesian and non-Cartesian sampling patterns, in which the undersampling pattern has higher dimensionality, and will study how such types of performance predictors along with training data sets, such as libraries of prototypical anatomical images, can improve prospective CS MRI acquisitions and reconstructions.

REFERENCES [1] Lustig et al.; *Mag Reson Med* 2007;58,1182-1195, [2] Goldstein, T., and Osher, S.; *SIAM J Imag Sci* 2009;2:323-343.

ACKNOWLEDGEMENTS NIBIB T32 EB001628, NCI 1U01CA142565, NCI 1R01CA129961.

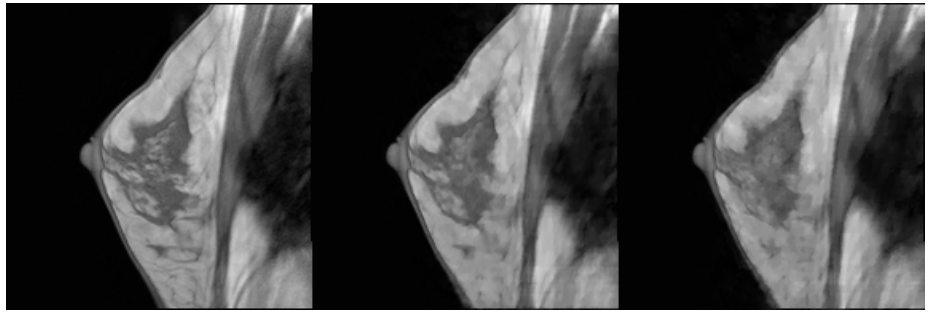


Fig. 1 – Example reconstructions: fully sampled (left) and CS reconstructions using 33% of the data and the masks with the highest (middle) and lowest (right) variance PSF. The highest variance PSF produced a superior image (middle) to the lowest variance PSF (right).

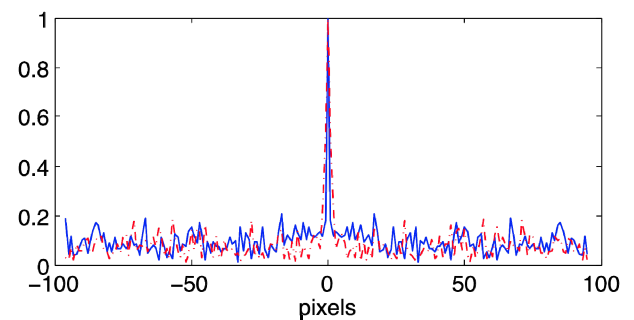


Fig. 2 – Fourier mask PSFs. Red is the largest variance PSF and blue is the lowest variance PSF. These PSFs are from the masks used in the middle and right images in Fig. 1.

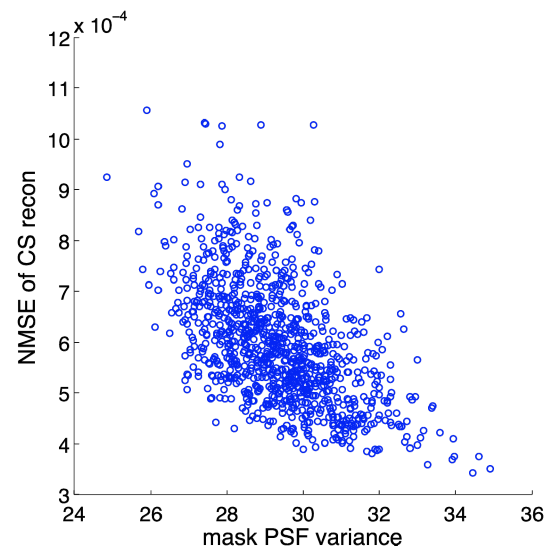


Fig. 3 – Reconstruction error as a function of random Fourier mask PSF. The highest variance PSFs produced consistently the most accurate reconstructions. The Spearman ρ for the trend is -0.55 ($p < 10^{-80}$).